

**TOWARD AN OPTIMIZED GLOBAL-IN-TIME SCHWARZ ALGORITHM
FOR DIFFUSION EQUATIONS WITH DISCONTINUOUS AND
SPATIALLY VARIABLE COEFFICIENTS.
PART 1: THE CONSTANT COEFFICIENTS CASE***

FLORIAN LEMARIÉ[†], LAURENT DEBREU[†], AND ERIC BLAYO[‡]

Abstract. In this paper we present a global-in-time non-overlapping Schwarz method applied to the one-dimensional unsteady diffusion equation. We address specifically the problem with discontinuous diffusion coefficients, our approach is therefore especially designed for subdomains with heterogeneous properties. We derive efficient interface conditions by solving analytically the minmax problem associated with the search for optimized conditions in a *Robin-Neumann* case and in a *two-sided Robin-Robin* case. The performance of the proposed schemes are illustrated by numerical experiments.

Key words. optimized Schwarz methods, waveform relaxation, alternating and parallel Schwarz methods

AMS subject classifications. 65M55, 65F10, 65N22, 35K15

1. Introduction. Numerous geophysical phenomena with a strong societal impact involve the coupled ocean-atmosphere system; e.g., those for climate change, tropical cyclones, or sea-level rise predictions. To get a good depiction of the complex air-sea dynamics, it is often necessary to couple atmospheric and oceanic simulation models. However, connecting the two model solutions at the air-sea interface is a difficult problem, which is presently often addressed in a simplified way from a mathematical point of view. Indeed, with the *ad-hoc* coupling methods currently in use, the fluxes exchanged by the two models are generally not in exact balance [17]. This may be one factor explaining the generally observed strong sensitivity of coupled solutions to the initial conditions or parameter values [23]. This kind of coupling raises a number of challenges in terms of numerical simulation since we are considering two highly turbulent fluids with widely different scales in time and space. It is thus natural to use some specific numerical treatment to match the physics of the two fluids at their interface. It is known that, even if numerical models are much more complicated, a simple one-dimensional diffusion equation is relevant to locally represent the turbulent mixing in the boundary layers encompassing the air-sea interface. The corresponding diffusion coefficients are spatially variable and their values are given by a so-called *eddy-viscosity* closure [21]. To perform this coupling in a more consistent way than *ad-hoc* methods, we propose here to adapt a global-in-time domain decomposition based on an optimized Schwarz method. This type of method is thoroughly described in [9] and designed thanks to the pioneering work in [12, 14]. Schwarz-like domain decomposition methods provide flexible and efficient tools for coupling models with non-conforming time and space discretizations [3, 10]. Transmission conditions of Robin type have been proposed in [19] to circumvent the inability of the classical Schwarz method (i.e., with the exchange of Dirichlet data) to solve coupling problems in the case of non-overlapping subdomains. Then, thanks to the free parameters in the Robin conditions, an optimization of the convergence speed has been proposed in [12, 15]: this is the basis of the so called *optimized Schwarz methods* (OSM). This kind of method, originally introduced for stationary problems, has been extended to the unsteady cases by adapt-

*Received September 29, 2010. Accepted March 11, 2013. Published online on July 5, 2013. Recommended by Martin Gander.

[†]INRIA Grenoble Rhône-Alpes, Montbonnot, 38334 Saint Ismier Cedex, France and Jean Kuntzmann Laboratory, BP 53, 38041 Grenoble Cedex 9, France, ({florian.lemarie, laurent.debreu}@inria.fr).

[‡]University of Grenoble, Jean Kuntzmann Laboratory, BP 53, 38041 Grenoble Cedex 9, France (eric.blayo@imag.fr).

ing the waveform relaxation algorithms to provide a *global-in-time Schwarz method* [14, 16] (sometimes referred to as *Schwarz waveform relaxation*). This notion of optimization of the convergence speed is critical in the context of ocean-atmosphere coupling as the numerical codes involved are very expensive from a computational point of view. In the present series of two papers, we derive interface conditions leading to an efficient Schwarz coupling algorithm between two unsteady diffusion equations defined on non-overlapping subdomains. The convergence properties of this kind of problem have already been extensively studied in the case of a constant diffusion coefficient having the same value in all subdomains [8]. There are some asymptotic results in the case of coefficients with different constant values in the different subdomains [10] (in the more general case of advection-diffusion-reaction equations). In the present papers, we extend these studies to the general case of diffusion coefficients which vary in each subdomain and whose values are different on both sides of the interface. In this first part, we consider the case of diffusion coefficients that do not vary spatially in each medium. We study a zeroth-order *two-sided* optimized method by considering two different Robin conditions on both sides of the interface. In the second paper [18], the emphasis is on the impact of the spatial variability of the coefficients on the convergence speed.

This first paper is organized as follows. In Section 2, we recall the basics of optimized Schwarz methods in the framework of time evolution problems. Sections 3 and 4 are dedicated to the study of a diffusion problem with discontinuous but piecewise constant coefficients. In Section 3, we analytically determine the solution of an optimization problem to improve the convergence speed of a simplified algorithm with only one Robin condition combined with a Neumann condition. In Section 4, we address the more general case of *two-sided* optimized Robin-Robin transmission conditions determined through a thorough study of the behavior of the convergence factor. Finally in Section 5, some numerical results are shown to prove the efficacy of the optimized algorithms derived in the previous sections.

2. Model problem and optimized Schwarz methods. Our guiding example is the one-dimensional diffusion equation of a scalar u

$$(2.1) \quad \mathcal{L}u = \partial_t u - \partial_x(D(x)\partial_x u) = f \quad \text{in } \Omega \times [0, T],$$

where Ω is a bounded domain defined as $\Omega =] -L_1, L_2[$, ($L_1, L_2 \in \mathbb{R}^+$) and $D(x) > 0$, for $x \in \Omega$. In practical applications, L_1 denotes the bottom of the ocean (of the order of 5 km in the open ocean), while L_2 is typically the top of the troposphere (of the order of 15 km). This problem is supplemented by an initial condition

$$u(x, 0) = u_0(x), \quad x \in \Omega,$$

and boundary conditions

$$\mathcal{B}_1 u(-L_1, t) = g_1, \quad \mathcal{B}_2 u(L_2, t) = g_2, \quad t \in [0, T],$$

where \mathcal{B}_1 and \mathcal{B}_2 are two partial differential operators. In this paper, we always assume that $u_0 \in H^1(\Omega)$, $f \in L^2(0, T; L^2(\Omega))$ and that $D(x)$ is bounded in the L^∞ -norm. Note that in actual applications such assumptions are generally fulfilled. Existence and uniqueness results for this problem can be proved following [10] and are not discussed here.

2.1. Formulation of the global-in-time Schwarz method. In the present study, we consider a case where the diffusion coefficient $D(x)$ has one discontinuity in Ω . This discontinuity represents the transition between two media with heterogeneous physical properties. In this case we define two subdomains, each subdomain having its own diffusion profile $D_j(x)$, ($j = 1, 2$). This amounts to splitting Ω into two non-overlapping domains Ω_1

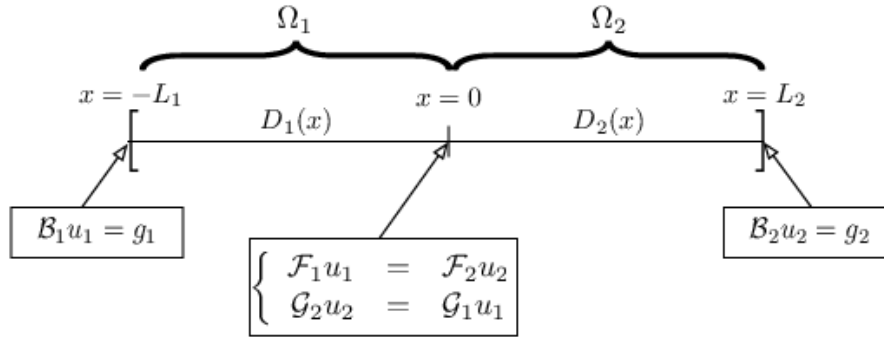


FIG. 2.1. Decomposition of the spatial domain Ω into two non-overlapping subdomains.

and Ω_2 ; see Figure 2.1. These subdomains communicate through their common interface at $\Gamma = \{x = 0\}$. (Note that there can be various reasons for such a splitting: different physics, parallelization and/or different numerical treatment requirements.) We propose to use a non-overlapping global-in-time Schwarz algorithm to solve the corresponding coupling problem. This method consists in iteratively solving subproblems in $\Omega_1 \times [0, T]$ and $\Omega_2 \times [0, T]$ using the values computed at the previous iteration in the other subdomain as an interface condition at $x = 0$. The operator \mathcal{L} introduced in (2.1) is split into two operators $\mathcal{L}_j = \partial_t - \partial_x(D_j(x)\partial_x)$ restricted to Ω_j ($j = 1, 2$). Introducing the operators $\mathcal{F}_1, \mathcal{F}_2, \mathcal{G}_1$, and \mathcal{G}_2 to define the interface conditions, the algorithm reads

$$\begin{aligned}
 (2.2) \quad & \begin{aligned}
 \mathcal{L}_1 u_1^k &= f, & \text{in } \Omega_1 \times [0, T], \\
 u_1^k(x, 0) &= u_o(x), & x \in \Omega_1, \\
 \mathcal{B}_1 u_1^k(-L_1, t) &= g_1, & t \in [0, T], \\
 \mathcal{F}_1 u_1^k(0, t) &= \mathcal{F}_2 u_2^{k-1}(0, t), & \text{in } \Gamma \times [0, T].
 \end{aligned} \\
 & \begin{aligned}
 \mathcal{L}_2 u_2^k &= f, & \text{in } \Omega_2 \times [0, T], \\
 u_2^k(x, 0) &= u_o(x), & x \in \Omega_2, \\
 \mathcal{B}_2 u_2^k(L_2, t) &= g_2, & t \in [0, T], \\
 \mathcal{G}_2 u_2^k(0, t) &= \mathcal{G}_1 u_1^k(0, t), & \text{in } \Gamma \times [0, T],
 \end{aligned}
 \end{aligned}$$

where $k = 1, 2, \dots$ is the iteration number, and where the initial guess $u_2^0(0, t)$ is given. Algorithm (2.2) corresponds to the so-called “multiplicative” form of the Schwarz method. If we replace the interface condition $\mathcal{G}_2 u_2^k = \mathcal{G}_1 u_1^k$ on Ω_2 by $\mathcal{G}_2 u_2^k = \mathcal{G}_1 u_1^{k-1}$, we obtain the “parallel” version of the algorithm. The multiplicative form converges more rapidly than the parallel one but prevents us from solving subproblems in parallel (this problem can, however, be circumvented when we consider more than two subdomains). The interested readers may refer to [7] for further details regarding the different variants of the Schwarz method. Although the present study uses the multiplicative form of the algorithm, the theoretical results regarding the determination of optimized transmission conditions are also valid for the parallel form. Note that the usual algorithmic approach used in ocean-atmosphere climate models as described in [4] generally corresponds to one (and only one) iteration of the algorithm in (2.2) (with $\mathcal{F}_j = \mathcal{G}_j = D_j(0)\partial_x$, $j = 1, 2$).

The primary role of the operators \mathcal{F}_j and \mathcal{G}_j ($j = 1, 2$) in (2.2) is to ensure a given consistency of the solution on the interface Γ . In our context we require the equality of the subproblems solutions and of their fluxes. The most natural choice to obtain such a

connection consists in choosing

$$\mathcal{F}_1 = D_1(0) \frac{\partial}{\partial x}, \quad \mathcal{F}_2 = D_2(0) \frac{\partial}{\partial x}, \quad \text{and} \quad \mathcal{G}_1 = \mathcal{G}_2 = Id.$$

However, as proposed in [19], the same consistency can be obtained using mixed boundary conditions of Robin type, leading to

$$(2.3) \quad \mathcal{F}_j = D_j(0) \frac{\partial}{\partial x} + \Lambda_1, \quad \text{and} \quad \mathcal{G}_j = D_j(0) \frac{\partial}{\partial x} + \Lambda_2 \quad (j = 1, 2).$$

The advantage of (2.3) is that if the operators Λ_1 and Λ_2 are correctly chosen, then we can greatly improve the convergence speed of the corresponding algorithm [12]. Note that Λ_j must also be carefully chosen to ensure the well-posedness of the problem. In this paper we focus on Robin-type transmission conditions since *Dirichlet-Neumann*-type algorithms generally converge quite slowly except for large discontinuities between the coefficients D_2 and D_1 . (It can easily be shown that the convergence rate is given by the square root of the ratio between D_1 and D_2 .)

At this point, we have formulated the coupling problem we want to address. The convergence properties of this kind of problem have been extensively studied in the case of constant and continuous diffusion coefficients [8]. There are also some results in the case of constant and discontinuous coefficients [10] in the more general case of an advection-diffusion-reaction problem. This latter study provides results for specific asymptotic cases that are discussed later in Section 4.4. In this paper, we propose to investigate the problem with diffusion coefficients being constant in each subdomain and discontinuous at the interface, i.e., $D_j(x) = D_j$, with $D_j > 0$ and $D_1 \neq D_2$. We prove convergence of the algorithm (2.2) and we determine optimal choices for the operators Λ_j under some constraints on the parameters of the problem.

2.2. Convergence of the algorithm. A classical approach to demonstrate the convergence of algorithm (2.2) consists of introducing the error e_j^k between the exact solution u^* and the iterates u_j^k , $j = 1, 2$. By linearity, those errors satisfy homogeneous diffusion equations with homogeneous initial conditions. We denote the Fourier transform in time by $\hat{g} = \mathcal{F}(g)$ for any $g \in L^2(\mathbb{R})$. Assuming that $T \rightarrow \infty$ and that all the functions are equal to zero for negative times, it can easily be shown that the errors \hat{e}_j^k in Fourier space satisfy a second-order ordinary differential equation in x

$$i\omega \hat{e}_j^k - D_j \frac{\partial^2 \hat{e}_j^k}{\partial x^2} = 0 \quad \text{for } x \in \Omega_j, \omega \in \mathbb{R}^*,$$

with characteristic roots $\sigma_j^\pm = \pm \sqrt{\frac{|\omega|}{2D_j}} \left(1 + \frac{|\omega|}{\omega} i\right)$. Note that the particular case $\omega = 0$ would correspond to the existence of a stationary part in the error. However, since the error is initially zero, such a stationary part is also necessarily zero. To study the convergence of algorithm (2.2), it is usually assumed that $L_1, L_2 \rightarrow \infty$, thus leading to

$$(2.4) \quad \begin{aligned} \hat{e}_1^k(x, \omega) &= \alpha^k(\omega) e^{\sigma_1^+ x}, & \text{for } x < 0, \omega \in \mathbb{R}^*, \\ \hat{e}_2^k(x, \omega) &= \beta^k(\omega) e^{\sigma_2^- x}, & \text{for } x > 0, \omega \in \mathbb{R}^*. \end{aligned}$$

The validity of this assumption is discussed in [17]. The functions $\alpha(\omega)$ and $\beta(\omega)$ are determined using the Robin interface conditions at $x = 0$

$$(2.5) \quad \begin{aligned} (D_1 \sigma_1^+ + \lambda_1) \alpha^k(\omega) &= (D_2 \sigma_2^- + \lambda_1) \beta^{k-1}(\omega), \\ (-D_2 \sigma_2^- + \lambda_2) \beta^k(\omega) &= (-D_1 \sigma_1^+ + \lambda_2) \alpha^k(\omega), \end{aligned}$$

where λ_j is defined as the *symbol* of the operator Λ_j ($j = 1, 2$). A convergence factor ρ of the Schwarz algorithm (2.2) can be defined as

$$\rho(\omega) = \left| \frac{\widehat{e}_1^k(0, \omega)}{\widehat{e}_1^{k-1}(0, \omega)} \right| = \left| \frac{\widehat{e}_2^k(0, \omega)}{\widehat{e}_2^{k-1}(0, \omega)} \right|.$$

Given (2.4), this amounts to $\rho(\omega) = |\alpha^k / \alpha^{k-1}| = |\beta^k / \beta^{k-1}|$. Using (2.5) we obtain

$$(2.6) \quad \rho(\omega) = \left| \frac{(\lambda_1(\omega) + D_2\sigma_2^-)(\lambda_2(\omega) - D_1\sigma_1^+)}{(\lambda_1(\omega) + D_1\sigma_1^+)(\lambda_2(\omega) - D_2\sigma_2^-)} \right|.$$

A more general derivation of the convergence factor for the case of an advection-diffusion-reaction problem with discontinuous coefficients can be found in [10]. At this point, we are not able to infer the convergence (or the divergence) of the corresponding algorithm because the operators Λ_j have not been explicitly determined. It is often a difficult task to choose them in an appropriate way. The main difficulty comes from the fact that the convergence factor is formulated in the Fourier space, meaning that we can only act on symbols λ_j and not directly on pseudo-differential operators Λ_j in the physical space.

2.3. The optimized Schwarz method. It is possible to find values λ_1 and λ_2 canceling the convergence factor (2.6) and therefore ensuring a convergence in exactly two iterations. Their expressions are

$$(2.7) \quad \lambda_1^{\text{opt}} = -D_2\sigma_2^- = \sqrt{\frac{|\omega|D_2}{2}}(1 + \frac{|\omega|}{\omega}i) \quad \text{and} \quad \lambda_2^{\text{opt}} = D_1\sigma_1^+ = \sqrt{\frac{|\omega|D_1}{2}}(1 + \frac{|\omega|}{\omega}i).$$

These symbols correspond to so-called *absorbing conditions*. Unfortunately, since these optimal symbols are not polynomials in $i\omega$, the absorbing conditions are nonlocal in time in the physical space. The problem is thus to determine local operators providing a good approximation of nonlocal ones by finding a polynomial form in $i\omega$ to approximate λ_j^{opt} . There are mainly two approaches for such an approximation [12]. The first approach is a low frequency approximation, namely a Taylor expansion for a small ω . We decided not to adopt this approach because we want to be able to consider a wide range of frequencies. The second and more sophisticated approach is to solve a minmax problem to determine local operators that optimize the convergence speed over the full range of admissible frequencies $[\omega_{\min}, \omega_{\max}]$. For a zeroth-order approximation, we look for values $\lambda_j^0 \in \mathbb{R}$ such that $\lambda_j^0 \approx \lambda_j^{\text{opt}}$. The numbers λ_j^0 can be defined as the solution of the optimization problem

$$(2.8) \quad \min_{\lambda_1^0, \lambda_2^0 \in \mathbb{R}} \left(\max_{\omega \in [\omega_{\min}, \omega_{\max}]} \rho(\lambda_1^0, \lambda_2^0, \omega) \right).$$

Since we work on a discrete problem, the frequencies allowed by our temporal grid range from $\omega_{\min} = \frac{\pi}{T}$ to $\omega_{\max} = \frac{\pi}{\Delta t}$, where Δt is the time step of the temporal discretization. The analytical solution of problem (2.8) is not an easy task: the minimization of a maximum is known to be one of the most difficult problems in optimization theory [5]. Moreover, we are faced with an optimization problem for two parameters λ_1^0 and λ_2^0 , which substantially enlarges the difficulty. Some analytical results exist in the case of a *two-sided* optimization for the 2D stationary diffusion equation [6, 20] and for the 2D Helmholtz equation [11]. In [10], the asymptotic solution of (2.8) for an advection-diffusion-reaction problem for $\Delta t \rightarrow 0$, $\omega_{\min} = 0$, and a positive advection is found in two particular cases: first for $\lambda_1^0 = \lambda_2^0$ (*one-sided*) and second for $\lambda_1^0 \neq \lambda_2^0$ (*two-sided*) but $D_1 = D_2$. In this paper, we

study the complete minmax problem (2.8) in the general case $\lambda_1^0 \neq \lambda_2^0$ and $D_1 \neq D_2$. Solving numerically the minmax problem (2.8) is quite expensive from a computational point of view. Moreover, this optimization must be performed for any change in the values of D_1 and D_2 . That is why we look for an analytical solution in the case of a zeroth-order approximation of the absorbing conditions. This is done with two different sets of interface conditions, the *Neumann-Robin* case and the *Robin-Robin* case.

Algorithm (2.2) with two-sided Robin conditions is well-posed for any choice of λ_1^0 and λ_2^0 such that $\lambda_1^0 + \lambda_2^0 > 0$. This result can be shown following the methodology based on a priori energy estimates as described in [1] and [8].

3. The optimized Schwarz method with Neumann-Robin interface conditions. In this section, we assume that the solution in Ω_2 is subject to a Neumann boundary condition. The convergence speed of the Neumann-Robin algorithm is expected to be slower than that one obtained by a Robin-Robin algorithm. However, this easier case is treated explicitly because it introduces several methodological aspects useful for the determination of the general Robin-Robin optimized interface conditions. Imposing a Neumann boundary condition on the solution u_2 on Γ corresponds to having $\Lambda_2 = 0$ in (2.3). The convergence factor ρ_{NR} (NR stands for “Neumann-Robin”) obtained from (2.6) reduces to

$$(3.1) \quad \rho_{\text{NR}} = \left| \frac{D_1 \sigma_1^+ (D_2 \sigma_2^- + \lambda_1)}{D_2 \sigma_2^- (D_1 \sigma_1^+ + \lambda_1)} \right|.$$

THEOREM 3.1 (Optimized Robin parameter). *The analytical solution $\lambda_1^{0,*}$ of the minmax problem*

$$\min_{\lambda_1^0 \in \mathbb{R}} \left(\max_{\omega \in [\omega_{\min}, \omega_{\max}]} \rho_{\text{NR}}(\lambda_1^0, D_1, D_2, \omega) \right)$$

is given by

$$\lambda_1^{0,*} = \frac{1}{2\sqrt{2}} \left\{ \left(\sqrt{D_2} - \sqrt{D_1} \right) (\sqrt{\omega_{\min}} + \sqrt{\omega_{\max}}) + \sqrt{\left(\sqrt{D_2} - \sqrt{D_1} \right)^2 (\sqrt{\omega_{\min}} + \sqrt{\omega_{\max}})^2 + 8\sqrt{D_1 D_2} \sqrt{\omega_{\min} \omega_{\max}}} \right\}.$$

Proof. Introducing $\zeta = \sqrt{|\omega|D_1}$, $\gamma = \sqrt{D_2/D_1}$, $\lambda_1^0 = \left(\sqrt{\zeta_{\min} \zeta_{\max}}/2 \right) p$, for $p \in \mathbb{R}$, and making σ_1^+ and σ_2^- in (3.1) explicit, we obtain

$$\rho_{\text{NR}}(p, \zeta) = \frac{1}{\gamma} \sqrt{\frac{(p - \gamma\zeta)^2 + \gamma^2 \zeta^2}{(p + \zeta)^2 + \zeta^2}},$$

with $\zeta = \zeta / \sqrt{\zeta_{\max} \zeta_{\min}}$. Moreover, to ensure the well-posedness of the algorithm, we consider $\lambda_1^0 > 0$, i.e., $p > 0$. Defining an additional parameter $\mu = \sqrt{\zeta_{\max}/\zeta_{\min}}$, we obtain that ζ is bounded by $\zeta_{\min} = \mu^{-1}$ and $\zeta_{\max} = \mu$. The aim is to optimize the convergence speed by finding p^* , the solution of the minmax problem

$$\min_{p > 0} \left(\max_{\zeta \in [\mu^{-1}, \mu]} \rho_{\text{NR}}(p, \zeta) \right).$$

We first study the behavior of the derivative of ρ_{NR} with respect to ζ and p with $\zeta \geq 0$ and $p \geq 0$. For simplicity we introduce $q = p / \left(\gamma - 1 + \sqrt{1 + \gamma^2} \right)$.

We first derive some restriction of the parameter's range. We can easily show that

$$(3.2) \quad \text{Sign} \left(\frac{\partial \rho_{\text{NR}}}{\partial p} \right) = \text{Sign} (q - \zeta).$$

Looking at the sign of the derivative of ρ_{NR} with respect to p , we see that for all values of ζ , the convergence factor ρ_{NR} is a decreasing function of p for $q < \zeta_{\min} = \mu^{-1}$, proving that $q^* \geq \zeta_{\min}$. A similar argument shows that $q^* \leq \zeta_{\max}$. This proves that the optimized parameter q^* satisfies

$$1/\mu \leq q^* \leq \mu.$$

Along with (3.2), this shows that the convergence factor has to be an increasing function of p at $\zeta = 1/\mu$ and a decreasing function of p at $\zeta = \mu$.

Next we show an equioscillation property of the optimal parameter. The sign of the derivative of ρ_{NR} with respect to ζ is given by

$$\text{Sign} \left(\frac{\partial \rho_{\text{NR}}}{\partial \zeta} \right) = \text{Sign} (\zeta - q).$$

This relation implies that ρ_{NR} has a local minimum between $1/\mu$ and μ . The maximum value of the convergence factor is thus attained either at $\zeta = 1/\mu$ or at $\zeta = \mu$ (or both). If we assume $\rho_{\text{NR}}(p, 1/\mu) < \rho_{\text{NR}}(p, \mu)$, it is always possible to decrease the maximum value of $\rho_{\text{NR}}(p, \zeta)$ by increasing the value of p so that we have $\rho_{\text{NR}}(p, 1/\mu) \geq \rho_{\text{NR}}(p, \mu)$. A similar argument shows that $\rho_{\text{NR}}(p, \mu) \geq \rho_{\text{NR}}(p, 1/\mu)$. The optimal parameter must thus satisfy the equioscillation property $\rho_{\text{NR}}(p^*, 1/\mu) = \rho_{\text{NR}}(p^*, \mu)$. After some simple algebra, we find that p^* is a solution of

$$(\gamma - 1)(\mu + 1/\mu) + \frac{2\gamma}{p^*} - p^* = 0.$$

The unique positive solution of the equation $v^* = \frac{2\gamma}{p^*} - p^*$ with $v^* = (1 - \gamma)(\mu + 1/\mu)$ is given by $p^* = \frac{1}{2} \left(-v^* + \sqrt{8\gamma + (v^*)^2} \right)$. After a substitution of γ and μ and a multiplication of p^* by $\sqrt{\zeta_{\min}\zeta_{\max}/2}$, we retrieve the stated result for $\lambda_1^{0,*}$. \square

We find that the optimized convergence factor satisfies an equioscillation property. This concept of equioscillation property comes from the Chebyshev's alternation theorem (or equioscillation theorem). The similarities between the Chebyshev's theorem and the optimized Schwarz method are clearly exposed in [2, 6]. Two typical optimized convergence factors $\rho_{\text{NR}}^* = \rho_{\text{NR}}(\lambda_1^{0,*})$ are shown in Figure 3.1 (left) for $\mu = 2$ and $\mu = 6$ with $\gamma = 5$. Note that the performance of the optimized algorithm is only a function of the ratio γ between D_1 and D_2 and not of the actual values of those parameters. The same remark applies to the temporal frequencies ω_{\min} and ω_{\max} : ρ_{NR}^* is only a function of their ratio μ .

It is also instructive to look at three particular cases: $\gamma \rightarrow 0^+$, $\gamma = 1$, and $\gamma \rightarrow \infty$.

- $\gamma \rightarrow 0^+$ ($D_1 \gg D_2$):

$$\lim_{\gamma \rightarrow 0^+} \rho_{\text{NR}}^* = \sqrt{1 - 2 \left(\frac{\mu}{1 + \mu^2} \right)^2}, \quad \lim_{\gamma \rightarrow 0^+} \lambda_1^{0,*} = 0, \quad \text{with } \mu = \left(\frac{\omega_{\max}}{\omega_{\min}} \right)^{1/4}.$$

The minimum value of the convergence factor is attained at $\mu = 1$ and is equal to $\sqrt{2}/2$. When μ is increased, the convergence is very slow. Indeed, we tend towards a Neumann-Neumann algorithm in this case.

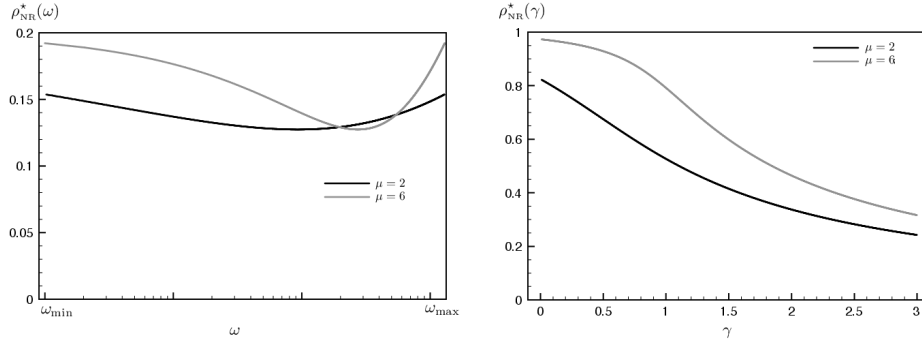


FIG. 3.1. Behavior of $\rho_{NR}(\lambda_1^{0,*})$ with respect to ω for $\gamma = 5$, $\mu = 2$, and $\mu = 6$ (left). Optimized convergence factor as a function of γ for $\mu = 2$ and $\mu = 6$ (right).

- $\gamma = 1$ ($D_1 = D_2 = D$):

$$\rho_{NR}^* = \sqrt{1 - \frac{2\sqrt{2}\mu}{1 + \mu(\mu + \sqrt{2})}}, \quad \lambda_1^{0,*} = \sqrt{D}(\omega_{\max}\omega_{\min})^{1/4}.$$

The convergence factor ρ_{NR}^* approaches 1 when μ is increased. One can also remark that the optimal parameter $\lambda_1^{0,*}$ is the same as that one found in [8] in the Robin-Robin one-sided case.

- $\gamma \rightarrow +\infty$ ($D_1 \ll D_2$):

$$\lim_{\gamma \rightarrow +\infty} \rho_{NR}^* = 0, \quad \lim_{\gamma \rightarrow +\infty} \lambda_1^{0,*} = +\infty.$$

When γ tends to $+\infty$, the convergence is very fast (the convergence factor approaches 0) and the optimal boundary condition tends towards a Neumann-Dirichlet operator.

These results are illustrated in Figure 3.1 (right). The efficiency of the Neumann-Robin algorithm is greatly improved when γ becomes large and μ becomes small. We continue this section by studying the asymptotic convergence rate for the discretized algorithm when the time step Δt tends to 0.

THEOREM 3.2 (Asymptotic performance). For $D_2 > D_1$ (i.e., $\gamma > 1$), $\omega_{\max} = \frac{\pi}{\Delta t}$ and for Δt tending to zero, the optimal Robin parameter given by Theorem 3.1 is

$$\lambda_1^{0,*} \approx \sqrt{2D_1} \left(\frac{\gamma - 1}{2} \sqrt{\pi} \Delta t^{-1/2} + \frac{\gamma^2 + 1}{2(\gamma - 1)} \sqrt{\omega_{\min}} \right)$$

and the asymptotic convergence of the optimized Neumann-Robin algorithm is

$$\max_{\omega_{\min} \leq \omega \leq \frac{\pi}{\Delta t}} \rho_{NR}(\lambda_1^{0,*}, \omega) = \frac{1}{\gamma} \left(1 - \frac{(\gamma + 1)}{(\gamma - 1)} \sqrt{\frac{\omega_{\min}}{\pi}} \Delta t^{1/2} \right) + O(\Delta t).$$

We conclude that the zeroth-order optimized Neumann-Robin boundary conditions are efficient when the Robin condition is imposed at the boundary of the domain with the smaller diffusion coefficient (Ω_1 here). In this case, the asymptotic convergence factor ρ_{NR}^* is of the form $\sqrt{D_1/D_2} (1 - O(\Delta t^{1/2}))$ for small Δt . In the next section, we study the zeroth-order two-sided Robin-Robin boundary conditions.

4. The optimized Schwarz method for a diffusion problem with discontinuous (but constant) coefficients: two-sided Robin transmission conditions. In this section we optimize the conditions on both sides of the interface to get a faster convergence speed regardless of the value of γ . By keeping the notations ζ , ζ , μ , and γ defined in the previous section and by approximating λ_1^{opt} and λ_2^{opt} respectively by $\lambda_1^0 = \sqrt{\frac{\zeta_{\min}\zeta_{\max}}{2}} p_2$ and $\lambda_2^0 = \sqrt{\frac{\zeta_{\min}\zeta_{\max}}{2}} p_1$, the convergence factor ρ_{RR} reads

$$\rho_{\text{RR}}(p_1, p_2, \zeta) = \sqrt{\frac{((p_1 - \zeta)^2 + \zeta^2) ((p_2 - \gamma\zeta)^2 + \gamma^2\zeta^2)}{((p_1 + \gamma\zeta)^2 + \gamma^2\zeta^2) ((p_2 + \zeta)^2 + \zeta^2)}}.$$

We can easily demonstrate that for nonnegative fixed values of ζ and γ and for $p_1, p_2 > 0$, we find the three inequalities $\rho_{\text{RR}}(p_1, p_2, \zeta) < \rho_{\text{RR}}(-p_1, -p_2, \zeta)$, $\rho_{\text{RR}}(p_1, p_2, \zeta) < \rho_{\text{RR}}(p_1, -p_2, \zeta)$, and $\rho_{\text{RR}}(p_1, p_2, \zeta) < \rho_{\text{RR}}(-p_1, p_2, \zeta)$. This shows that we can restrict our study to strictly positive values of p_1 and p_2 (note that $p_1 = 0$ or $p_2 = 0$ corresponds to the *Neumann-Robin* case). The restriction of the parameter range to strictly positive values ensures that $\lambda_1^0 + \lambda_2^0 > 0$, and hence the corresponding problem is well-posed. In the following, we assume that $\gamma \geq 1$. The optimal parameters p_1 and p_2 for the case $\gamma \leq 1$ can be obtained by switching (i.e. p_1 becomes p_2 and p_2 becomes p_1) the optimal values for the case $\gamma \geq 1$. As it was done previously, we choose the values p_1 and p_2 by solving the optimization problem

$$(4.1) \quad \min_{p_1, p_2 > 0} \left(\max_{\zeta \in [\mu^{-1}, \mu]} \rho_{\text{RR}}(p_1, p_2, \zeta) \right).$$

4.1. Behavior of the convergence factor with respect to the Robin parameters. First, we study the behavior of ρ_{RR} with respect to the parameters p_1 and p_2 . We introduce two new parameters q_1 and q_2 defined by

$$q_1 = \frac{p_1}{1 - \gamma + \sqrt{1 + \gamma^2}} \quad \text{and} \quad q_2 = \frac{p_2}{\gamma - 1 + \sqrt{1 + \gamma^2}}.$$

We can demonstrate that for $\gamma \geq 1$ and $q_1 \leq q_2$, we have that $\rho_{\text{RR}}(p_1, p_2, \zeta) \leq \rho_{\text{RR}}(p_2, p_1, \zeta)$. This proves that the optimal parameters satisfy $q_1^* \leq q_2^*$. This implies that in turn $p_1 \leq p_2$ and that $p_1 < p_2$ if $\gamma > 1$. This immediately proves that *one-sided* ($p_1 = p_2$) Robin-Robin boundary conditions are not optimal as soon as $\gamma > 1$.

Note that $\text{Sign}\left(\frac{\partial \rho_{\text{RR}}}{\partial p_1}\right) = \text{Sign}(q_1 - \zeta)$ and $\text{Sign}\left(\frac{\partial \rho_{\text{RR}}}{\partial p_2}\right) = \text{Sign}(q_2 - \zeta)$ implies

$$(4.2) \quad \begin{aligned} \frac{\partial \rho_{\text{RR}}}{\partial p_1} > 0 & \quad \text{when } \zeta < q_1, & \quad \frac{\partial \rho_{\text{RR}}}{\partial p_1} < 0 & \quad \text{when } \zeta > q_1, \\ \frac{\partial \rho_{\text{RR}}}{\partial p_2} > 0 & \quad \text{when } \zeta < q_2, & \quad \frac{\partial \rho_{\text{RR}}}{\partial p_2} < 0 & \quad \text{when } \zeta > q_2. \end{aligned}$$

Looking at the signs of the derivatives of ρ_{RR} with respect to p_1 and p_2 , we find that if we choose $q_1 < \zeta_{\min} = \mu^{-1}$, we can decrease the convergence factor by increasing p_1 because $\frac{\partial \rho_{\text{RR}}}{\partial p_1} < 0$ holds for all $q_1 > \zeta_{\min}$. A similar argument shows that $q_2 \leq \zeta_{\max}$. This means that the optimized parameters q_1^* and q_2^* must satisfy

$$(4.3) \quad \mu^{-1} \leq q_1^* < q_2^* \leq \mu.$$

The inequalities (4.2) and (4.3) imply that at $\zeta = 1/\mu$, ρ_{RR} is an increasing function of p_1 and p_2 (or q_1 and q_2) while at $\zeta = \mu$, ρ_{RR} is a decreasing function of p_1 and p_2 (or q_1 and q_2).

4.2. Extrema of ρ_{RR} with respect to ζ . The next step to solve (4.1) analytically is to find the location of the extrema of $\rho_{RR}(p_1, p_2, \zeta, \gamma)$ with respect to ζ .

THEOREM 4.1 (Extrema of $\rho_{RR}(\zeta)$). *The function $\zeta \rightarrow \rho_{RR}(p_1, p_2, \zeta)$ has one or three positive local extrema. In the case of one extremum, it corresponds to a minimum and is located at $\zeta = \chi := \sqrt{\frac{p_1 p_2}{2\gamma}}$.*

Proof. We first introduce the following property that can easily be verified:

$$\rho_{RR}(p_1, p_2, \zeta) = \rho_{RR}(p_1, p_2, \chi^2/\zeta), \text{ where } \chi = \sqrt{\frac{p_1 p_2}{2\gamma}}.$$

Differentiating with respect to ζ leads to

$$(4.4) \quad \frac{\partial \rho_{RR}}{\partial \zeta}(p_1, p_2, \zeta) = -\frac{\chi^2}{\zeta^2} \frac{\partial \rho_{RR}}{\partial \zeta}(p_1, p_2, \chi^2/\zeta),$$

which shows that $\frac{\partial \rho_{RR}}{\partial \zeta}(p_1, p_2, \pm\chi) = 0$. The derivative $\frac{\partial \rho_{RR}(p_1, p_2, \zeta)}{\partial \zeta}$ has the same sign as a (unitary) sixth-order polynomial $P(\zeta)$ (the full expression of P is complicated and not given here). $P(\zeta)$ has thus either two or six real roots, among them $\zeta = \chi$ is positive and $\zeta = -\chi$ is negative. Let us suppose that $P(\zeta)$ has six real roots. We can show that only three of these six roots (including $\zeta = \chi$) are positive. From (4.4) we see that if ζ^0 is a root of $P(\zeta)$, then $\zeta^1 = \chi^2/\zeta^0$ is another one. Assuming that the four other roots are positive, we have

$$\zeta_5 = -\chi \leq 0 \leq \zeta_6 \leq \zeta_1 \leq \zeta_2 = \chi \leq \zeta_3 (= \frac{\chi^2}{\zeta_1}) \leq \zeta_4 (= \frac{\chi^2}{\zeta_6}),$$

and the sum of the six roots must be greater than 2χ and is therefore positive. However, the sum of the six roots of $P(\zeta)$ is given by $-a_5$ where a_5 is the coefficient of the term ζ^5 and is equal to $a_5 = \frac{(\gamma-1)(p_2-p_1)}{\gamma}$. Using the facts $\gamma \geq 1$ and $p_2 \geq p_1$ (from (4.3)), $-a_5$ cannot be positive. We conclude that we have at most three positive roots for $P(\zeta)$. It can be verified that $P(0) < 0$ and $P(+\infty) > 0$ so that if only one positive root exists (at $\zeta = \chi$), it is a local minimum. \square

4.3. Equioscillation of ρ_{RR} at the end points.

THEOREM 4.2 (Equioscillation at the end points). *The optimized convergence factor $\rho_{RR}(p_1^*, p_2^*, \zeta)$ satisfies*

- $\rho_{RR}(p_1^*, p_2^*, \chi) \leq \max(\rho_{RR}(p_1^*, p_2^*, \mu^{-1}), \rho_{RR}(p_1^*, p_2^*, \mu))$ with $\chi = \sqrt{\frac{p_1^* p_2^*}{2\gamma}}$,
- the equioscillation property $\rho_{RR}(p_1^*, p_2^*, \mu^{-1}) = \rho_{RR}(p_1^*, p_2^*, \mu)$, which holds only for $p_1^* p_2^* = 2\gamma$.

Proof. We first show that $\rho_{RR}(p_1^*, p_2^*, \chi) \leq \max(\rho_{RR}(p_1^*, p_2^*, \mu^{-1}), \rho_{RR}(p_1^*, p_2^*, \mu))$. This is straightforward when χ is the only positive root of $\frac{\partial \rho_{RR}(\zeta)}{\partial \zeta}$ because χ is a local minimum. In the case when there are three positive roots, χ is a local maximum. From the identity $\chi = \sqrt{\frac{p_1 p_2}{2\gamma}} = \sqrt{q_1 q_2}$ and (4.3), we get

$$(4.5) \quad 1/\mu \leq q_1 \leq \chi = \sqrt{q_1 q_2} \leq q_2 \leq \mu.$$

We already know that at $\zeta = 1/\mu$, ρ_{RR} is a decreasing function of q_1 and that at $\zeta = \mu$, ρ_{RR} is an increasing function of q_1 . The inequality (4.5) shows that at $\zeta = \chi$, ρ_{RR} is an increasing function of q_1 since $q_1 \leq \chi$. If we assume that $\rho_{RR}(p_1^*, p_2^*, \chi) \geq \rho_{RR}(p_1^*, p_2^*, \mu^{-1})$, then we can always decrease q_1 (or p_1) such that it improves the convergence factor (by reducing the values both at $\zeta = \chi$ and at $\zeta = \mu$). Playing with q_2 , we can similarly prove

that $\overline{\rho_{\text{RR}}}(p_1^*, p_2^*, \chi) \leq \rho_{\text{RR}}(p_1^*, p_2^*, \mu)$. Note that this also proves that $\zeta_1 \geq 1/\mu$ and $\zeta_3 \leq \mu$. This is sufficient to fully describe the behavior of the convergence factor with respect to q_1 , q_2 , and ζ , as shown in Figure 4.1. In practice, the two cases will differ by the sign of the second-order derivative of $\rho_{\text{RR}}(p_1, p_2, \zeta)$ at $\zeta = \chi$. The following argument proves that the values taken by $\rho_{\text{RR}}(p_1^*, p_2^*, \zeta)$ at the two end points $\zeta = 1/\mu$, and $\zeta = \mu$ are equal. Indeed, if we assume that $\rho_{\text{RR}}(p_1, p_2, 1/\mu) < \rho_{\text{RR}}(p_1, p_2, \mu)$ (or $\rho_{\text{RR}}(p_1, p_2, 1/\mu) > \rho_{\text{RR}}(p_1, p_2, \mu)$) holds, it is always possible to decrease the maximum value of $\rho_{\text{RR}}(\zeta)$ by increasing (respectively decreasing) the values of p_1 (respectively p_2). The optimal parameters must thus satisfy the equioscillation property $\rho_{\text{RR}}(p_1^*, p_2^*, \mu^{-1}) = \rho_{\text{RR}}(p_1^*, p_2^*, \mu)$. This holds when

$$(4.6) \quad (p_1 + p_2)(2\gamma - p_1 p_2)S(p_1, p_2, \mu, \gamma) = 0,$$

where

$$\begin{aligned} S(p_1, p_2, \mu, \gamma) &= 2 [(1 + \gamma^2) - \gamma(\mu + \mu^{-1})^2] p_1 p_2 \\ &\quad + (\gamma - 1)(\mu + 1/\mu)(p_1 - p_2)(2\gamma + p_1 p_2) \\ &\quad + 2\gamma(p_1 - p_2)^2 - (2\gamma - p_1 p_2)^2. \end{aligned}$$

Obviously every pair (p_1, p_2) that satisfies the relation $p_1 p_2 = 2\gamma$ is a solution to (4.6). We now show that there are no other admissible values. Other potential solutions of the problem are the solutions of $S(p_1, p_2, \mu) = 0$. S is a second-order polynomial in p_2 and thus has two real solutions:

$$(4.7) \quad p_2 = f_1(p_1), \quad p_2 = f_2(p_1).$$

If we assume that p_2 is related to p_1 with one of the relations (4.7), looking at Figure 4.1, we can argue that for any pair (p_1, p_2) we must have $\frac{dp_2}{dp_1} < 0$ to satisfy an equioscillation property. Indeed, let $\rho_{\text{RR}}^\dagger(p_1, \zeta)$ be defined as

$$\rho_{\text{RR}}^\dagger(p_1, \zeta) = \rho_{\text{RR}}(p_1, p_2(p_1), \zeta).$$

Then

$$(4.8) \quad \frac{\partial \rho_{\text{RR}}^\dagger(p_1, \zeta)}{\partial p_1} = \frac{\partial \rho_{\text{RR}}(p_1, p_2(p_1), \zeta)}{\partial p_1} + \frac{\partial \rho_{\text{RR}}(p_1, p_2(p_1), \zeta)}{\partial p_2} \frac{dp_2}{dp_1}.$$

We have already proved that the following properties must hold

$$(4.9) \quad \begin{aligned} \frac{\partial \rho_{\text{RR}}(p_1, p_2(p_1), 1/\mu)}{\partial p_1} &> 0, & \frac{\partial \rho_{\text{RR}}(p_1, p_2(p_1), 1/\mu)}{\partial p_2} &> 0, \\ \frac{\partial \rho_{\text{RR}}(p_1, p_2(p_1), \mu)}{\partial p_1} &< 0, & \frac{\partial \rho_{\text{RR}}(p_1, p_2(p_1), \mu)}{\partial p_2} &< 0. \end{aligned}$$

If we suppose $\frac{dp_2}{dp_1} > 0$, then (4.8) and (4.9) show that $\rho_{\text{RR}}^\dagger(p_1, 1/\mu)$ is an increasing function of p_1 while $\rho_{\text{RR}}^\dagger(p_1, \mu)$ is a decreasing function of p_1 . Hence, (4.9) and the equioscillation property cannot be satisfied at the same time if $\frac{dp_2}{dp_1} > 0$. It can be shown that the two solutions given by (4.7) do not satisfy this latter condition. Indeed, we can prove that we have $\frac{df_1}{dp_1} > 0$ and $\frac{df_2}{dp_1} > 0$. Details of the computations are omitted here but we mention that the only conditions necessary to find this result are $\gamma > 0, \mu > 1$. We can conclude that $p_1 p_2 = 2\gamma$ is the only solution leading to an equioscillation property. \square

It is worth mentioning that $\chi = \sqrt{\frac{p_1 p_2}{2\gamma}} = 1$ and that

$$\rho_{\text{RR}}(p_1^*, p_2^*, \zeta) = \rho_{\text{RR}}(p_1^*, p_2^*, 1/\zeta), \quad \forall \zeta \in [1/\mu, \mu].$$

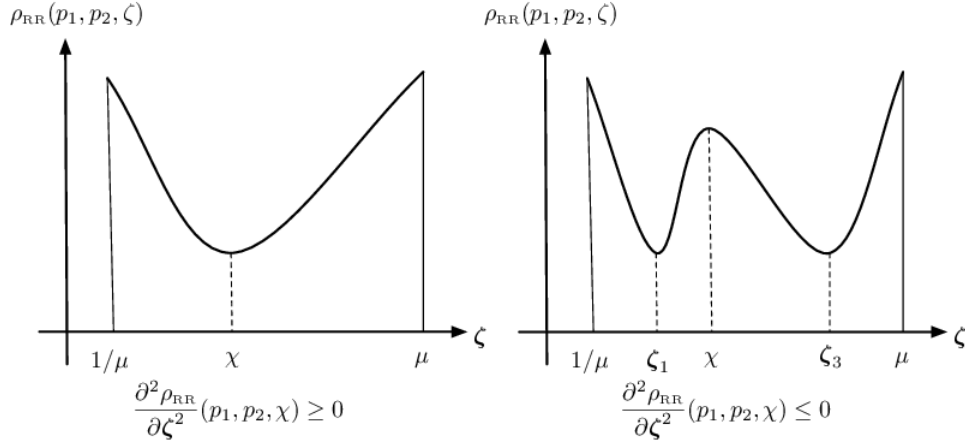


FIG. 4.1. Behavior of the convergence factor with respect to ζ .

4.4. Solution of the minmax problem. The convergence factor is now a function of p_1 and ζ only:

$$\rho_{RR}^\dagger(p_1, \zeta) = \rho_{RR}(p_1, 2\gamma/p_1, \zeta).$$

LEMMA 4.3. *The solution of the minmax problem (4.1) is given by the solution of the constraint minimization problem*

$$\min_{p_1^* \geq p_1^{*,\text{equi}}} \rho_{RR}^\dagger(p_1^*, 1/\mu),$$

where $p_1^{*,\text{equi}}$ is the solution of the three-point equioscillation problem

$$\rho_{RR}^\dagger(p_1, 1) = \rho_{RR}^\dagger(p_1, 1/\mu) = \rho_{RR}^\dagger(p_1, \mu).$$

Proof. Thanks to Figure 4.1, we can remark that the resolution of the minmax problem corresponds to the minimization of $\rho_{RR}^\dagger(p_1, 1/\mu)$ (or $\rho_{RR}^\dagger(p_1, \mu)$) with respect to p_1 . In the case where $\chi = 1$ is a local maximum, the additional constraint given by Theorem 4.2 must be imposed

$$(4.10) \quad \rho_{RR}^\dagger(p_1, 1) \leq \rho_{RR}^\dagger(p_1, 1/\mu).$$

Knowing that $p_1 p_2 = 2\gamma$ or equivalently $q_1 q_2 = 1$, the range of admissible values given by the inequality (4.3) can now be written as $1/\mu \leq q_1 \leq 1$ and translates in terms of the variable p_1 :

$$(4.11) \quad p_1 \in [p_{1,\min}, p_{1,\max}], \text{ where } p_{1,\min} = (1 - \gamma + \sqrt{1 + \gamma^2})/\mu, \quad p_{1,\max} = (1 - \gamma + \sqrt{1 + \gamma^2}).$$

Moreover, it can be shown that $\rho_{RR}^\dagger(p_1, 1)$ is a decreasing function of p_1 and therefore the constraint (4.10) can also be written as $p_1^* \geq p_1^{*,\text{equi}}$ where $p_1^{*,\text{equi}}$ is the solution of a three-point equioscillation problem $\rho_{RR}^\dagger(p_1^{*,\text{equi}}, 1) = \rho_{RR}^\dagger(p_1^{*,\text{equi}}, 1/\mu) (= \rho_{RR}^\dagger(p_1^{*,\text{equi}}, \mu))$. \square

We now look at the minimization of $\rho_{RR}^\dagger(p_1, 1/\mu)$ for $p_1 \in [p_{1,\min}, p_{1,\max}]$.

LEMMA 4.4. *For $\gamma > 1$, the derivative of $\rho_{RR}^\dagger(p_1, 1/\mu)$ has exactly one root in the range $[p_{1,\min}, p_{1,\max}]$. This root corresponds to a local minimum of $\rho_{RR}^\dagger(p_1, 1/\mu)$. In the special case $\gamma = 1$, $p_1 = p_{1,\max} (= \sqrt{2})$ is always a root of $\frac{\partial \rho_{RR}^\dagger}{\partial p_1}(p_1, 1/\mu)$.*

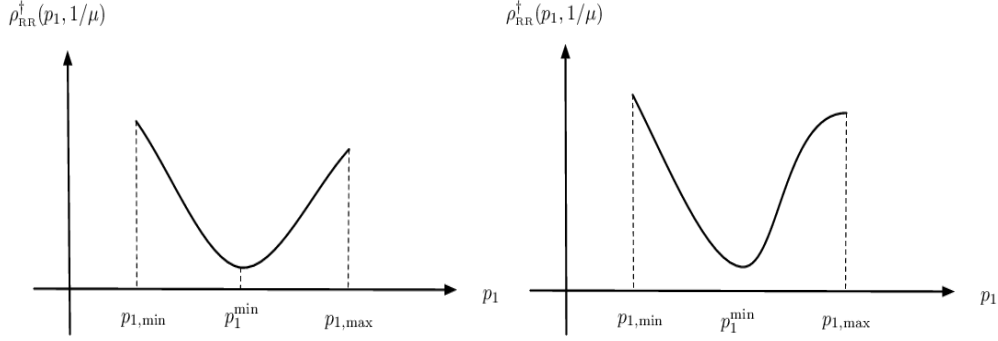


FIG. 4.2. Behavior of $\rho_{\text{RR}}^\dagger(p_1, 1/\mu)$ with respect to p_1 . The general case ($\gamma > 1$) is on the left and the special case $\gamma = 1$ on the right.

Proof. The derivative of $\rho_{\text{RR}}^\dagger(p_1, 1/\mu)$ can be written as

$$\frac{\partial \rho_{\text{RR}}^\dagger}{\partial p_1}(p_1, 1/\mu) = g(p_1, \mu)N(p_1, \mu),$$

where g is a strictly positive function and $N(p_1, \mu)$ a sixth-order polynomial in p_1 . The change of variable $v = 2\gamma/p_1 - p_1$ transforms $N(p_1, \mu)$ into

$$N(p_1, \mu) = p_1^3 Q(v),$$

where $Q(v)$ is the third-order polynomial given by

$$(4.12) \quad Q(v) = 8(\gamma - 1)(1 + \gamma^2) + 2\beta(\gamma\beta^2 - 3(1 + \gamma^2))v + 2(\gamma - 1)\beta^2 v^2 - \beta v^3,$$

with $\beta = 1/\mu + \mu$.

It can be shown that, for $\gamma > 1$, this polynomial has only one root in $[v_{\min}, v_{\max}]$, where, according to (4.11), v_{\min} and v_{\max} are given by

$$v_{\min} = 2(\gamma - 1), \quad v_{\max} = (\gamma - 1)\beta + \sqrt{1 + \gamma^2} \sqrt{\beta^2 - 4}.$$

This root corresponds to a minimum of the functional $\rho_{\text{RR}}^\dagger(p_1, 1/\mu)$ because we can show that $\frac{\partial \rho_{\text{RR}}^\dagger}{\partial p_1}(p_{1,\min}, 1/\mu) \leq 0$ and $\frac{\partial \rho_{\text{RR}}^\dagger}{\partial p_1}(p_{1,\max}, 1/\mu) \geq 0$. For $\gamma = 1$, the value $v = v_{\min} = 0$, i.e., $p_1 = p_{1,\max} = \sqrt{2}$, is always a root of $Q(v)$. Figure 4.2 illustrates the variations of $\rho_{\text{RR}}^\dagger(p_1, 1/\mu)$ with respect to p_1 . p_1^{\min} is the location of the minimum of $\rho_{\text{RR}}^\dagger(p_1, 1/\mu)$ over the interval $[p_{1,\min}, p_{1,\max}]$. The solution of the constrained minimization problem is now easily handled: if $p_1^{\min} \leq p_1^{*,\text{equi}}$, then the solution of the minmax problem is given by $p_1^{*,\text{equi}}$, otherwise the solution of the minmax problem is given by p_1^{\min} .

The inequality $p_1^{\min} \leq p_1^{*,\text{equi}}$ is satisfied if and only if $\frac{\partial \rho_{\text{RR}}^\dagger}{\partial p_1}(p_1^{*,\text{equi}}, \mu) \geq 0$ or equivalently if $Q(v^{*,\text{equi}}) \geq 0$, where $v^{*,\text{equi}} = 2\gamma/p_1^{*,\text{equi}} - p_1^{*,\text{equi}}$.

Finally, the following result is useful: for $v \geq v_{\max}$ (or equivalently $p_1 \leq p_{1,\min}$), we have $Q(v) \leq 0$ (or $\frac{\partial \rho_{\text{RR}}^\dagger(p_1, 1/\mu)}{\partial p_1} \leq 0$). Indeed, using the relation (4.8) at $\zeta = 1/\mu$, we obtain

$$\frac{\partial \rho_{\text{RR}}^\dagger(p_1, 1/\mu)}{\partial p_1} = \frac{\partial \rho_{\text{RR}}(p_1, p_2(p_1), 1/\mu)}{\partial p_1} + \frac{\partial \rho_{\text{RR}}(p_1, p_2(p_1), 1/\mu)}{\partial p_2} \frac{dp_2}{dp_1}.$$

If $p_1 \leq p_{1,\min}$ holds, then we get $\frac{\partial \rho_{RR}(p_1, p_2(p_1), 1/\mu)}{\partial p_1} < 0$, but the relation $p_2 = 2\gamma/p_1$ implies that $p_2 \geq p_{2,\max} \left(= \left(\gamma - 1 + \sqrt{1 + \gamma^2} \right) \mu \right)$ so that $\frac{\partial \rho_{RR}(p_1, p_2(p_1), 1/\mu)}{\partial p_2} \geq 0$. With the help of $\frac{dp_2}{dp_1} = -2\gamma/p_1^2 \leq 0$, this proves that $\frac{\partial \rho_{RR}^\dagger(p_1, 1/\mu)}{\partial p_1} \leq 0$. \square

We are now finished with the problem of finding the solution of the three-point equioscillation problem.

THEOREM 4.5 (Equioscillation between three points). *The only parameters $p_1^{*,\text{equi}}$ and $p_2^{*,\text{equi}}$, such that $p_1^{*,\text{equi}} \leq p_{1,\max}$, that satisfy an equioscillation of the convergence factor ρ_{RR} between the three points $(1/\mu, 1, \mu)$ are*

$$\begin{aligned} p_1^{*,\text{equi}} &= \frac{1}{2} \left[-v^{*,\text{equi}} + \sqrt{8\gamma + (v^{*,\text{equi}})^2} \right], \\ p_2^{*,\text{equi}} &= 2\gamma \left(p_1^{*,\text{equi}} \right)^{-1}, \end{aligned}$$

where

$$(4.13) \quad v^{*,\text{equi}} = \frac{1}{2} \left[(2 + \beta)(\gamma - 1) + \sqrt{4(1 + \gamma)^2(\beta - 1) + \beta^2(\gamma - 1)^2} \right].$$

Proof. We have to find the solution of the problem $\rho_{RR}^\dagger(p_1, 1/\mu) = \rho_{RR}^\dagger(p_1, 1)$. It can be shown that this is equivalent to the search for the roots of a fourth-order polynomial $R(p_1)$ that can be written as

$$R(p_1) = p_1^2 T(v), \quad T(v) = 2(1 + \gamma^2) - 4\gamma\beta + (1 - \gamma)(2 + \beta)v + v^2,$$

where v is again defined by $v = 2\gamma/p_1 - p_1$. The unique root of $T(v)$ that satisfies $v \geq v_{\min}$ (i.e., $p_1 \leq p_{1,\max}$) is given by

$$v^{*,\text{equi}} = \frac{1}{2} \left[(2 + \beta)(\gamma - 1) + \sqrt{4(1 + \gamma)^2(\beta - 1) + \beta^2(\gamma - 1)^2} \right],$$

and the expression for $p_1^{*,\text{equi}}$ is deduced from the relation between p_1 and v . \square

Gathering the results, the solution of the minmax problem is given in the following theorem.

THEOREM 4.6. *The analytical solution $\lambda_1^{0,*}$ and $\lambda_2^{0,*}$ of the minmax problem*

$$\min_{\lambda_1^0, \lambda_2^0 \in \mathbb{R}} \left(\max_{\omega \in [\omega_{\min}, \omega_{\max}]} \rho_{RR}(\lambda_1^0, \lambda_2^0, D_1, D_2, \omega) \right)$$

is given by

$$\begin{aligned} \lambda_1^{0,*} &= \frac{\sqrt{D_1} (\omega_{\min} \omega_{\max})^{1/4}}{2\sqrt{2}} \left[-v^* + \sqrt{8\gamma + (v^*)^2} \right], \\ \lambda_2^{0,*} &= \sqrt{D_1 D_2} \sqrt{\omega_{\min} \omega_{\max}} / \lambda_1^{0,*}, \end{aligned}$$

where

$$v^* = \begin{cases} v^{*,\text{equi}} & \text{if } Q(v^{*,\text{equi}}) \geq 0, \\ v^{*,\text{mini}} & \text{else,} \end{cases}$$

with $v^{*,\text{equi}}$ given by (4.13) and $v^{*,\text{mini}}$ is the unique solution of $Q(v) = 0$ in $[v_{\min}, v_{\max}]$.

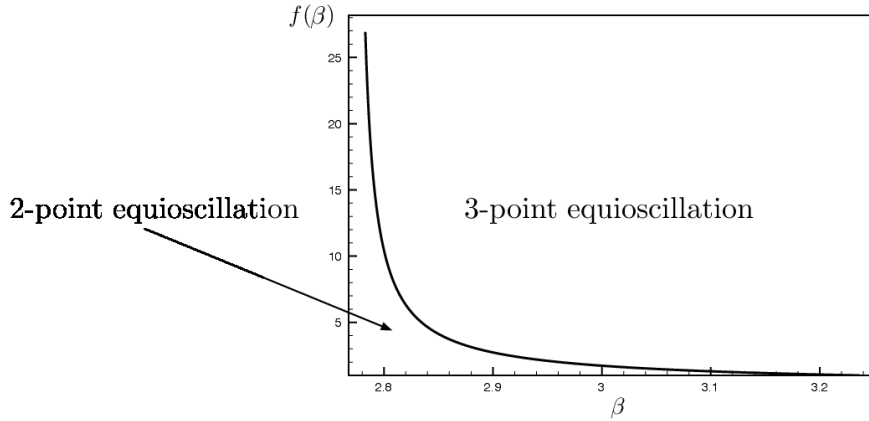


FIG. 4.3. Transition from a two-point to a three-point equioscillation for $\beta^0 < \beta < 1 + \sqrt{5}$. The three-point equioscillation occurs when $\gamma \geq f(\beta)$.

Proof. All the ingredients for the proof are stated before. Note that $v^{*,\text{equi}}$ may be larger than v_{\max} . However, since we have proved that $Q(v \geq v_{\max}) \leq 0$, this case does not have to be considered explicitly. A substitution of γ and μ by their respective expressions, and a multiplication of p_1^* and p_2^* by $\sqrt{\zeta_{\min}\zeta_{\max}}/2$ lead to the result for $\lambda_1^{0,*}$ and $\lambda_2^{0,*}$ with respect to D_1, D_2, ω_{\min} , and ω_{\max} . \square

Note that the following additional result can be shown as well:

$$(4.14) \quad Q(v^{*,\text{equi}}) \geq 0 \Leftrightarrow \beta \geq 1 + \sqrt{5} \text{ or } \left(\beta^0 < \beta < 1 + \sqrt{5} \text{ and } \gamma \geq f(\beta) \right),$$

where β^0 is the root of the fourth-order polynomial $16 - 16X - 4X^2 + X^4$ whose approximate value is given by $\beta^0 \approx 2.77294$ and f is given by

$$f(\beta) = \frac{1}{16 - 16\beta - 4\beta^2 + \beta^4} \left((\beta - 2)^3 \beta (\beta + 2) + (4 + 2\beta - \beta^2) \sqrt{-16 + 48\beta - 44\beta^2 + 12\beta^3 + 3\beta^4 - 4\beta^5 + \beta^6} \right).$$

The function $f(\beta)$ is plotted in Figure 4.3 for $\beta^0 < \beta < 1 + \sqrt{5}$. We remark that $f(\beta) \geq 1$ for all β so that the condition $\gamma \geq f(\beta)$ is always false for $\gamma = 1$ (the continuous case).

It is also interesting to know if $\chi = \sqrt{\frac{p_1 p_2}{2\gamma}} = 1$ is either a local minimum or a local maximum of the optimized convergence factor by looking at the sign of $\frac{\partial^2 \rho_{\text{RR}}^\dagger}{\partial \chi^2}(p_1, \chi)$. It can be proved that in terms of the variable $v = 2\gamma/p_1 - p_1$, the inequality $\frac{\partial^2 \rho_{\text{RR}}^\dagger}{\partial \chi^2}(p_1, \chi) > 0$ can be written as

$$v \geq v_0, \quad \text{where } v_0 = 2(\gamma - 1) + \sqrt{2(1 + \gamma^2)}.$$

We deduce that $\zeta = \chi = 1$ is a local minimum only if $v^{*,\text{mini}} \leq v_0$. This can be verified by evaluating the polynomial $Q(v)$ at $v = v_0$ and looking at the sign of the result: if $Q(v_0) \leq 0$, then $v^{*,\text{mini}} \leq v_0$ and we have a local minimum at $\zeta = \chi = 1$.

It can be found that

$$Q(v_0) < 0 \Leftrightarrow 2 < \beta < \beta_0 \quad \text{or } \left(\beta_0 \leq \beta \leq 2\sqrt{2} \text{ and } \gamma < g(\beta) \right),$$

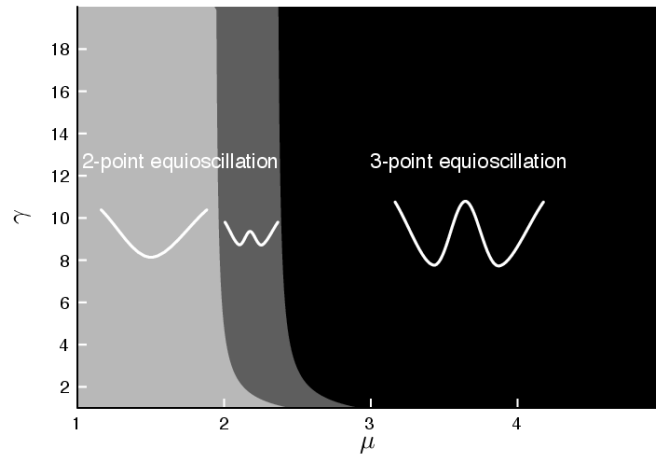


FIG. 4.4. The three different domains of three-point equioscillation (black), two-point equioscillation with χ being a local maximum (dark grey) and two-point equioscillation with χ being a local minimum (light grey).

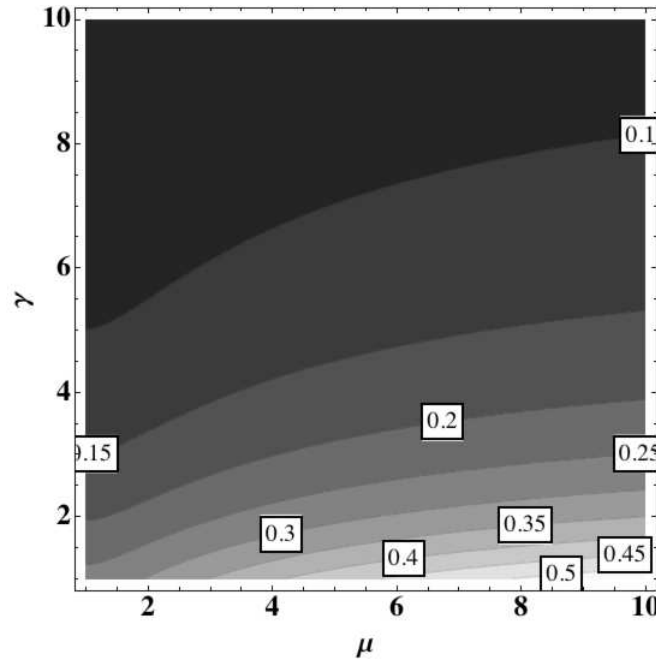


FIG. 4.5. Optimized convergence factor with respect to μ and γ ($1 \leq \mu \leq 10, 1 \leq \gamma \leq 10$).

where $\beta_0 = \frac{8+5\sqrt{2}}{2(3+2\sqrt{2})} + \frac{\sqrt{90+64\sqrt{2}}}{2(3+2\sqrt{2})} \approx 2.44547$. The analytical expression of $g(\beta)$ is complicated and not given here. Note that $g(\beta) \geq 1$ for all β so that for the special case $\gamma = 1$, the inequality $Q(v_0) < 0$ is equivalent to $2 < \beta \leq 2\sqrt{2}$.

Figure 4.4 summarizes the three different domains: three-point equioscillation, two-point equioscillation with χ as a local maximum and two-point equioscillation with χ as a local minimum. The resulting optimized convergence factor is shown in Figure 4.5 with respect to μ and γ .

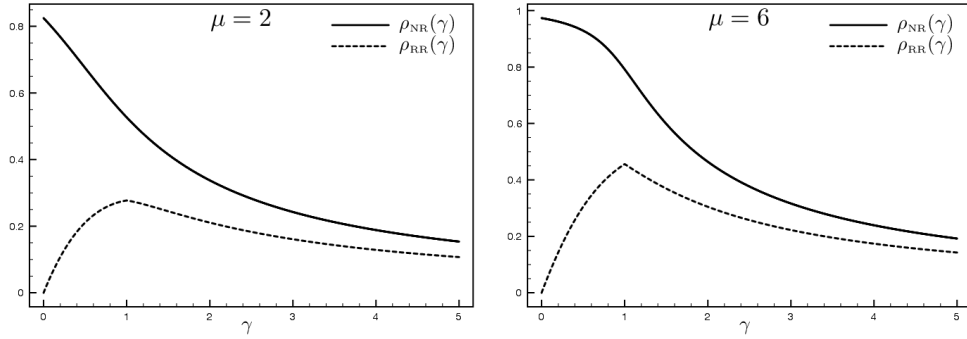


FIG. 4.6. Optimized convergence factors for Neumann-Robin and Robin-Robin boundary conditions for $\mu = 2$ (left) and $\mu = 6$ (right).

We make the following remarks about the convergence properties of the Schwarz algorithms: the convergence speed increases when the discontinuities of the coefficients (γ) is increased and the convergence speed decreases when μ , an increasing function of the ratio $\frac{\omega_{\max}}{\omega_{\min}}$, is increased. In Figure 4.6 we compare, for $\mu = 2$ and $\mu = 6$, the results found in the optimized two-sided case with the optimized Robin-Neumann transmission conditions (found in Section 3). The Robin-Robin approach is significantly more efficient than the Robin-Neumann approach when γ is close to one. When γ is increased, both tend towards a Dirichlet-Neumann operator.

THEOREM 4.7 (Asymptotic performance). For $D_2 > D_1$ (i.e., $\gamma > 1$), $\omega_{\max} = \frac{\pi}{\Delta t}$, and for Δt tending to zero, the optimal Robin parameters given by Theorem 4.6 are

$$\lambda_1^{0,*} \approx \lambda_1^{0,(as)} = \sqrt{2D_1} \left(\frac{\gamma}{\gamma-1} \sqrt{\omega_{\min}} - 2\gamma \frac{\gamma^2+1}{(\gamma-1)^3 \pi^{1/4}} \omega_{\min}^{3/4} \Delta t^{1/4} \right),$$

$$\lambda_2^{0,*} \approx \lambda_2^{0,(as)} = \sqrt{2D_1} \left(\frac{\gamma-1}{2} \sqrt{\pi} \Delta t^{-1/2} + \frac{\gamma^2+1}{\gamma-1} (\pi \omega_{\min})^{1/4} \Delta t^{-1/4} \right),$$

and the asymptotic convergence of the optimized two-sided Robin-Robin algorithm is

$$\max_{\omega_{\min} \leq \omega \leq \frac{\pi}{\Delta t}} \rho_{RR}(\lambda_1^{0,*}, \lambda_2^{0,*}, \omega) = \frac{1}{\gamma} \left(1 - 2 \frac{(\gamma+1)}{(\gamma-1)} \left(\frac{\omega_{\min}}{\pi} \right)^{1/4} \Delta t^{1/4} \right) + O(\Delta t^{1/2}).$$

Note that these asymptotic results are obtained by assuming that $v^* = v^{*,\text{equi}}$, which is always the case when $\Delta t \rightarrow 0$ (i.e., $\mu \rightarrow \infty$), as shown by (4.14). The optimized Robin-Robin conditions lead to an asymptotic convergence factor $\sqrt{D_1/D_2} (1 - O(\Delta t^{1/4}))$ for small Δt and $D_1 < D_2$. The associated algorithm is thus less sensitive to Δt than the Neumann-Robin algorithm. However, the asymptotic Robin parameters given in Theorem 4.7 must be used with caution as they degenerate when $\gamma \rightarrow 1$ as well as when $\Delta t \gg 0$ (in this case $\lambda_1^{0,(as)}$ can become negative). It is worth mentioning that the asymptotic bound on the optimized convergence factor given in Theorem 4.7 shows that the optimized Robin-Robin conditions will always be more efficient than Dirichlet-Neumann conditions. Indeed, it can easily be checked that the multiplicative factor $1/\gamma$ in front of the bound corresponds to the convergence factor of the Dirichlet-Neumann algorithm.

Furthermore, we can not directly compare this result with the one obtained in [10] for the advection-diffusion-reaction equation. The latter study is done by assuming $\omega_{\min} = 0$ and as a result of this assumption their optimized parameters, when canceling the advection and reaction coefficients, are simply $\lambda_1^{0,*} = \lambda_2^{0,*} = 0$. Indeed, one can easily find that for

a diffusion problem, the low frequency approximation λ_j^{low} of the absorbing conditions λ_j^{opt} given in (2.7) for $\omega_{\min} \rightarrow 0$ is indeed $\lambda_j^{\text{low}} = 0$.

4.5. The continuous case. Because the two-sided Robin-Robin case with continuous diffusion coefficients has never been studied in the literature, we now provide the results in this particular case.

THEOREM 4.8 (Continuous case). *Under the assumption $D_1 = D_2 = D$, the optimal parameters $\lambda_1^{0,*}$ and $\lambda_2^{0,*}$ are given by*

$$\lambda_1^{0,*} = \frac{\sqrt{D} (\omega_{\min} \omega_{\max})^{1/4}}{2\sqrt{2}} \left[-v^* + \sqrt{8 + (v^*)^2} \right]$$

$$\lambda_2^{0,*} = \frac{\sqrt{D} (\omega_{\min} \omega_{\max})^{1/4}}{2\sqrt{2}} \left[v^* + \sqrt{8 + (v^*)^2} \right]$$

where

$$v^* = \begin{cases} 2\sqrt{\beta - 1} & \text{if } \beta \geq 1 + \sqrt{5} \\ \sqrt{2\beta^2 - 12} & \text{if } \sqrt{6} \leq \beta < 1 + \sqrt{5} \\ 0 & \text{if } 2 < \beta < \sqrt{6} \end{cases}$$

$$\text{with } \beta = \frac{\sqrt{\omega_{\max}} + \sqrt{\omega_{\min}}}{(\omega_{\min} \omega_{\max})^{1/4}}.$$

Proof. We use Theorem 4.6, which gives the optimality conditions in the general case. As already mentioned, the condition $Q(v^{*,\text{equi}}) \geq 0$ reduces to $\beta \geq 1 + \sqrt{5}$ for $\gamma = 1$. In that case, the solution of the minmax problem is given by $v^* = v^{*,\text{equi}} = 2\sqrt{\beta - 1}$. If $\beta < 1 + \sqrt{5}$, we have to compute $v^{*,\text{min}}$, the value that cancels $Q(v)$ in $[v_{\min}, v_{\max}]$, where $v_{\min} = 0$, $v_{\max} = 2\sqrt{\beta^2 - 4}$. For $\gamma = 1$, the expression (4.12) of the polynomial $Q(v)$ is

$$Q(v) = -\beta v (v^2 - (2\beta^2 - 12)).$$

We find that

$$v^{*,\text{min}} = \begin{cases} \sqrt{2\beta^2 - 12}, & \text{if } \beta \geq \sqrt{6}, \\ 0, & \text{if } 2 < \beta \leq \sqrt{6}. \end{cases}$$

Note that when $\beta \leq \sqrt{6}$, we get $v^* = 0$. This implies $\lambda_1^{0,*} = \lambda_2^{0,*} = \sqrt{D_1} (\omega_{\min} \omega_{\max})^{1/4}$, which corresponds to the zeroth-order *one-sided* optimal parameters found in [8]. \square

5. Numerical experiments with two subdomains. The model problem (2.2) is discretized using a backward Euler scheme in time and a second-order scheme on a staggered grid in space. For the interior points, the scheme is

$$\frac{u_k^{n+1} - u_k^n}{\Delta t} = \frac{1}{x_{k+\frac{1}{2}} - x_{k-\frac{1}{2}}} \left[\mathbb{F}_{k+\frac{1}{2}}^{n+1} - \mathbb{F}_{k-\frac{1}{2}}^{n+1} \right],$$

with $\mathbb{F}_{k+\frac{1}{2}}^n = D_{k+\frac{1}{2}} \frac{u_{k+1}^n - u_k^n}{x_{k+1} - x_k}$. Note that for practical applications, the use of the Crank-Nicolson scheme in time is avoided because this leads to unphysical behavior. Indeed, unlike the backward Euler scheme, the Crank-Nicolson scheme fails to satisfy the so-called

monotonic damping property [22]. We decompose the computational domain Ω into two non-overlapping subdomains $\Omega_1 = [-L_1, 0]$ and $\Omega_2 = [0, L_2]$, with $L_1 = L_2 = 500$ m. A homogeneous Neumann boundary condition is imposed at $x = -L_1$ and $x = L_2$. As it is usually done in numerical models, the resolution Δx_k is progressively refined to enhance the resolution in the boundary layers in the vicinity of the air-sea interface. We use $N = 75$ points in each subdomain and the resolution varies from $\Delta x_k = 25$ m at $x = L_1$ (respectively $x = L_2$) to $\Delta x_k = 1$ m at $x = 0$. The Robin condition $g_{N+\frac{1}{2}}$ on the interface Γ (located at $x = x_{N+\frac{1}{2}}$ on Ω_1 and at $x = x_{\frac{1}{2}}$ on Ω_2) is discretized by assuming that the flux F is constant on the first cell near Γ . This leads to

$$g_{N+\frac{1}{2}} = D_{N-\frac{1}{2}} \frac{u_N - u_{N-1}}{x_{N-\frac{1}{2}} - x_{N-\frac{3}{2}}} + \lambda u_N,$$

where λ is the Robin parameter. We simulate directly the error equations, i.e., $f_1 = f_2 = 0$ in (2.2) and $u_0(x) = 0$. We start the iteration with a random initial guess $u_2^0(0, t)$, $t \in [0, T]$, so that it contains a wide range of the temporal frequencies that can be resolved by the computational grid. We perform simulations for four different types of transmission conditions at $x = 0$: Dirichlet-Neumann (DN), optimized Neumann-Robin (NR*), optimized Robin-Robin (RR*), and asymptotically optimized Robin-Robin (RR^(as)). In Figure 5.1 we show the evolution of the \mathcal{L}^∞ -norm of the error obtained for those four cases for $\gamma = 10^{\frac{1}{4}} \approx 1.7783$, $\gamma = \sqrt{10} \approx 3.1623$, and $\gamma = 10$, with $\mu = 6$ and $\mu = 12$. We choose the time steps $\Delta t_1 = \Delta t_2 = \Delta t = 100$ s, $D_2 = 0.5 \text{ m}^2\text{s}^{-1}$, and D_1 is then deduced depending on the value of γ . As expected, we get the best results with the two-sided Robin conditions. Consistent with Figure 4.5, the convergence is faster when γ is large and when μ is small. Moreover, when the discontinuity γ between the diffusion coefficients is increased, the algorithm becomes less and less sensitive to the choice of transmission conditions and to the parameter μ . The asymptotic optimized Robin-Robin conditions provide a good approximation of the optimized Robin-Robin conditions, even for $\Delta t = 100$ s $\gg 0$. Those conditions are especially efficient when γ is sufficiently larger than 1. We remark that the optimized Neumann-Robin conditions provide only a slight improvement compared to the classical Dirichlet-Neumann conditions.

Because we consider a problem with discontinuous coefficients, the time step used to advance the diffusion equation may be different in each subdomain. It is thus instructive to look at the impact of non-conformities in time on the performance of the optimized algorithm. For the two cases $\gamma = 10^{\frac{1}{4}}$ and $\gamma = 10$, which we considered so far, we adapt the time step in each subdomain so that the ratio $r = \Delta t_1/\Delta t_2$ between the time steps varies from 100 to 1/100. To handle the exchange of boundary data between the non-conforming grids we use a linear method for the interpolation step and an averaging for the restriction step, both steps are conservative. Note that we got very similar results using the \mathcal{L}^2 projection algorithm described in [13, Appendix A]. We consider $\omega_{\max} = \pi/\min(\Delta t_1, \Delta t_2)$ for the optimization of the Robin conditions.

As shown in Figure 5.2, the performance of the algorithm is degraded as long as $r \neq 1$. Indeed, the interpolation/restriction step modifies the frequency spectrum of the error and thus affects the convergence speed of the algorithm. For the cases $r \neq 1$, we have investigated a wide range of values for the parameters p_j in the Robin transmission conditions. Even if the algorithm is slower than the one with $r = 1$, it turned out that the optimal Robin parameters found in Theorem 4.6 are still optimal in the case $r \neq 1$. Note that the results after one iteration can be quite dependent on the value of r . This is to be expected since the frequency spectrum in the initial error is very different whether the (random) initial guess is initialized on the grid with the smaller time step or the larger time step.

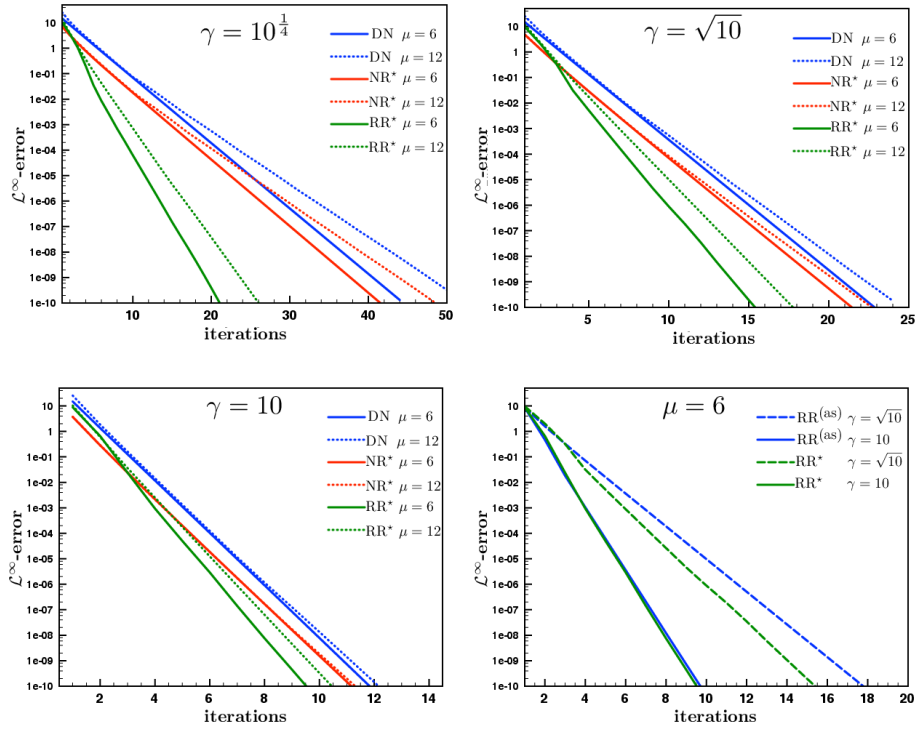


FIG. 5.1. Convergence for $\gamma = 10^{\frac{1}{4}}$ (top, left), $\gamma = \sqrt{10}$ (top, right), and $\gamma = 10$ (bottom, left) for $\mu = 6$ and $\mu = 12$ in the DN, RR^* , and NR^* cases. Comparison between RR^* and $RR^{(as)}$ (bottom, right).

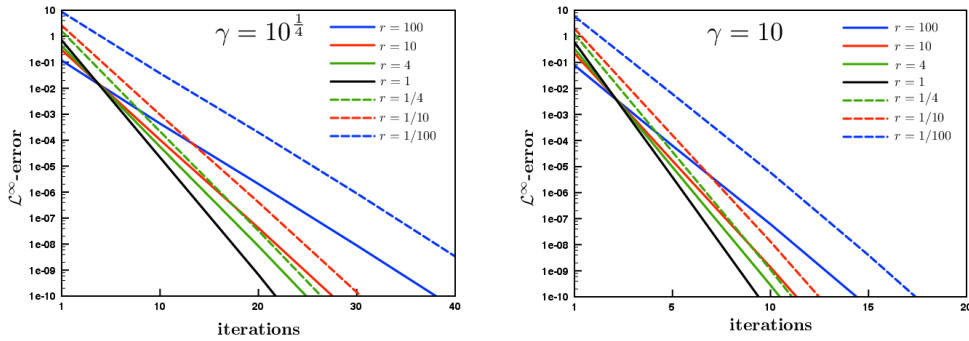


FIG. 5.2. Convergence for $\gamma = 10^{\frac{1}{4}}$ (left) and $\gamma = 10$ (right) for different values of the ratio $r = \Delta t_1 / \Delta t_2$ with $\mu = 6$ in the RR^* case.

Conclusion. In this paper, we obtain new results for an optimized Schwarz method defined for non-overlapping diffusion problems with discontinuous coefficients. This method uses zeroth-order two-sided Robin transmission conditions, i.e., we consider two different Robin conditions on each side of the interface. We base our approach on a model problem with two subdomains and we prove the convergence of the corresponding algorithm. Then we analytically study the behavior of the convergence factor with respect to the parameters of the problem. We show that the optimized convergence factor satisfies an equioscillation property between two or three points depending on the parameter values. In comparison with other methods using the Neumann-Robin or Dirichlet-Neumann conditions, these two-sided

Robin-Robin conditions are significantly more efficient, especially when the ratio between the discontinuous coefficients is close to one. Asymptotic results for Δt small are given. Numerical results show the performance of the different type of transmission conditions introduced in this paper. Those results are consistent with the analytical study.

Acknowledgements. This research was partially supported by the French National Research Agency (ANR) project "COMMA" and by the INRIA project-team MOISE. The authors would also like to thank two anonymous reviewers, whose comments and suggestions during the review process helped to clarify earlier version of the manuscript.

REFERENCES

- [1] D. BENNEQUIN, M. GANDER, AND L. HALPERN, *Optimized Schwarz waveform relaxation methods for convection reaction diffusion problems*, Technical Report 2004-24, LAGA, Université Paris 13, 2004.
- [2] ———, *A homographic best approximation problem with application to optimized Schwarz waveform relaxation*, *Math. Comp.*, 78 (2009), pp. 185–223.
- [3] E. BLAYO, L. HALPERN, AND C. JAPHET, *Optimized Schwarz waveform relaxation algorithms with nonconforming time discretization for coupling convection-diffusion problems with discontinuous coefficients*, in *Domain Decomposition Methods in Science and Engineering XVI*, O. Widlund and D. E. Keyes, eds., *Lect. Notes Comput. Sci. Eng.*, 55, Springer, Berlin, 2007, pp. 267–274.
- [4] G. DANABASOGLU, W. G. LARGE, J. J. TRIBBIA, P. R. GENT, B. P. BRIEGLEB, AND J. C. MCWILLIAMS, *Diurnal coupling in the tropical oceans of CCSM3*, *J. Climate*, 19 (2006), pp. 2347–2365.
- [5] V. F. DEM'YANOV AND V. N. MALOZEMOV, *On the theory of non-linear minimax problems*, *Russian Math. Surveys*, 26 (1971), pp. 57–115.
- [6] O. DUBOIS, *Optimized Schwarz Methods for the Advection-Diffusion Equation and for Problems with Discontinuous Coefficients*, Ph.D. Thesis, Dept. of Math. and Stat., McGill University, Montreal, 2007.
- [7] M. J. GANDER, *Schwarz methods over the course of time*, *Electron. Trans. Numer. Anal.*, 31 (2008), pp. 228–255. <http://etna.math.kent.edu/vol.31.2008/pp228-255.dir>
- [8] M. J. GANDER AND L. HALPERN, *Méthodes de relaxation d'ondes pour l'équation de la chaleur en dimension 1*, *C. R. Acad. Sci. Paris*, 336 (2003), pp. 519–524.
- [9] ———, *Optimized Schwarz waveform relaxation methods for advection reaction diffusion problems*, *SIAM J. Numer. Anal.*, 45 (2007), pp. 666–697.
- [10] M. J. GANDER, L. HALPERN, AND M. KERN, *A Schwarz waveform relaxation method for advection-diffusion-reaction problems with discontinuous coefficients and non-matching grids*, in *Domain Decomposition Methods in Science and Engineering XVI*, O. Widlund and D. E. Keyes, eds., *Lect. Notes Comput. Sci. Eng.*, 55, Springer, Berlin, 2007, pp. 283–290.
- [11] M. J. GANDER, L. HALPERN, AND F. MAGOULÈS, *An optimized Schwarz method with two-sided Robin transmission conditions for the Helmholtz equation*, *Internat. J. Numer. Methods Fluids*, 55 (2007), pp. 163–175.
- [12] M. J. GANDER, L. HALPERN, AND F. NATAF, *Optimal convergence for overlapping and non-overlapping Schwarz waveform relaxation*, in *Eleventh International Conference on Domain Decomposition Methods London 1998*, C. H. Lai, P. E. Bjørstad, M. Cross, and O. Widlund, eds., *DDM.org*, Augsburg, 1999, pp. 27–36.
- [13] ———, *Optimal Schwarz waveform relaxation for the one dimensional wave equation*, *SIAM J. Numer. Anal.*, 41 (2003), pp. 1643–1681.
- [14] M. J. GANDER AND A. M. STUART, *Space-time continuous analysis of waveform relaxation for the heat equation*, *SIAM J. Sci. Comput.*, 19 (1998), pp. 2014–2031.
- [15] C. JAPHET AND F. NATAF, *The best interface conditions for domain decomposition methods: absorbing boundary conditions*, in *Absorbing Boundaries and Layers, Domain Decomposition Methods*, L. Tourrette and L. Halpern, eds., *Nova Sci. Publ.*, Huntington, NY, 2001, pp. 348–373.
- [16] E. LELARASMEE, A. RUEHLI, AND A. SANGIOVANNI-VINCENTELLI, *The waveform relaxation method for time-domain analysis of large scale integrated circuits*, *IEEE Trans. Computer-Aided Design Integr. Circuits Syst.*, 1 (1982), pp. 131–145.
- [17] F. LEMARIÉ, *Algorithmes de Schwarz et couplage océan-atmosphère*, Ph.D. Thesis, Laboratoire Jean Kuntzmann, Joseph Fourier University, Grenoble, 2008.
- [18] F. LEMARIÉ, L. DEBREU, AND E. BLAYO, *Toward an optimized global-in-time Schwarz algorithm for diffusion equations with discontinuous and spatially variable coefficients. Part 2: the variable coefficients case*, *Electron. Trans. Numer. Anal.*, 40 (2013), pp. 170–186. <http://etna.math.kent.edu/vol.40.2013/pp170-186.dir>
- [19] P.-L. LIONS, *On the Schwarz alternating method. III. A variant for nonoverlapping subdomains*, in *Third In-*

- ternational Symposium on Domain Decomposition Methods for Partial Differential Equations, T. Chan, R. Glowinski, J. Periaux, and O. Widlund, eds., SIAM, Philadelphia, 1990, pp. 202–223.
- [20] Y. MADAY AND F. MAGOULÈS, *Non-overlapping additive Schwarz methods tuned to highly heterogeneous media*, C. R. Math. Acad. Sci. Paris, 341 (2005), pp. 701–705.
- [21] O. S. MADSEN, *A realistic model of the wind-induced Ekman boundary layer*, J. Phys. Oceanogr., 7 (1977), pp. 248–255.
- [22] G. MANFREDI AND M. OTTAVIANI, *Finite-difference schemes for the diffusion equation*, in Dynamical Systems, Plasmas and Gravitation, P. Leach, S. Bouquet, J.-L. Rouet, and E. Fijalkow, eds., Lecture Notes in Physics, 518, Springer, Berlin, 1999, pp. 82–92.
- [23] J. C. MCWILLIAMS, *Irreducible imprecision in atmospheric and oceanic simulations*, Proc. Natl. Acad. Sci. USA, 104 (2007), pp. 8709–8713.